Adsorption of Bemacid Red by Poly Tetra (Ethylene Glycol) Dimethacrylate Crosslinked with 2-Hydroxypropyl Methacrylate Hydrogels: Equilibrium and Kinetic Studies

Asmahane Fasla[1,2*], Zoubida Seghier[1], Abdelkader Iddou[3], and Laura Caserta[4]

[1]*Laboratory of Macromolecular Physical Chemistry, Faculty of Exact and Applied Sciences, Oran 1 Ahmed Benbella El Mnaouer University, Oran, Algeria*

[2]*Department of Chemistry, Faculty of Science, of Science and Technology University, Oran, El Mnaouer, Oran, Algeria*

[3]*Laboratory of Materials Recovery and Nuisance Treatment, Mostaganem University, Mostaganem, Algeria*

[4]*Catalysis-Master Park Company, Marseille, France*

Corresponding author:

tel: +213-771820794
email: afasla2005@yahoo.fr

Received: October 4, 2021
Accepted: March 8, 2022

DOI: 10.22146/ijc.69548

Abstract: *Besides others, textile industries are the primary sources of discharging a massive amount of highly colored wastewater. Adsorption can be considered the most economically favorable technology method for removing dyes from wastewater. This paper reports the synthesis of Poly tetra (ethyleneglycol) dimethacrylate crosslinked with 2-hydroxypropyl methacrylate (Poly (TtEGDMA-cross-2-HPMA)) hydrogels and its application as a novel sorbent to remove bemacid red (ET_2) dye from aqueous solution under various operating conditions. The equilibrium adsorption capacity was found 142.82–883.60 mg ET_2 g^{-1} of 1% TtEGDMA. The adsorbent was characterized using Fourier transform infrared radiation (FTIR) and ^{13}carbon solid-state nuclear magnetic resonance spectra (^{13}C-NMR). The effects of the experimental parameters include dye concentration and crosslinked agent concentration. The kinetic sorption uptake for ET_2 by Poly (TtEGDMA-cross-2-HPMA) at various initial dye concentrations was analyzed by pseudo-first and pseudo-second models. Two sorption isotherms, namely the Langmuir and Freundlich isotherms, were applied to the sorption equilibrium data. The sorption kinetics of ET_2 onto the hydrogels followed the pseudo-second-order kinetics model (R^2 = 0.999) and the adsorption equilibrium data obeyed the Langmuir isotherm model (R^2 = 0.999). It can be concluded that Poly (TtEGDMA-cross-2-HPMA) is an alternative economic sorbent to more costly adsorbents used for dye removal in wastewater treatment processes.*

Keywords: *tetra (ethylene glycol) dimethacrylate; 2-hydroxypropyl methacrylate; bemacid red; pseudo-second model; Langmuir isotherm*

■ INTRODUCTION

More than 10,000 dyes have been widely used in textile, paper, rubber, plastics, leather, cosmetics, pharmaceutical, and food industries to color their products, which generates a huge volume of wastewater every year [1-2]. The disposal of dye wastewater without proper treatment is a big challenge and has caused harm to the aquatic environment, such as reducing light penetration and photosynthesis [1]. Some of the dyes contained in wastewater are decomposed into carcinogenic aromatic amines under anaerobic conditions, which could cause serious health problems to humans and animals [1]. Dyes prevent light from penetrating water masses and suppress the photosynthesis process. Thus, the biological energy flow in the water environment is affected. Due to the carcinogenic and mutagenic properties of the dyes, they also affect microbial and other living organisms in water [3].

Due to the low biodegradability, conventional biological wastewater treatment processes are not

efficient in treating dyes wastewater [1]. Therefore, dye wastewater is usually treated by physical, chemical, and biological processes [3-4]. Due to its cost-effectiveness, simple design, and ease of use, adsorption is the most preferred method for physical-chemical wastewater treatment [3,5-7]. Several adsorbents have been reported in the literature, such as clay such as smectites [8-10], zeolite [11-13], fly ash [10,14-15], silica gel [16-18], chitosan [9,19], and algae [20-21] regarding the adsorption of basic dyes from aqueous solution. Several methods were developed for wastewater treatment [21-24].

Adsorption is the best process, the most comprehensive technique [25], the most effective process of advanced wastewater treatment employed to reduce hazardous pollutants present in the effluent [21,26-27], the most economical and effective way to eliminate many types of contaminants [21].

The major advantages of adsorption over conventional treatment methods include; low operating cost [21,28-32], simplicity of implementation [21,28-31], affordability [28-31], ease of operation [32], high efficiency [21,28-32], minimization of chemical or biological sludge [32], no additional nutrient requirement [32], regeneration of biosorbent [32], possibility of sorbate recovery [32], and reusability of the adsorbent [28-31].

Hydrogels with three-dimensional crosslinking networks can be used to treat printing and dyeing wastewater with simple operations efficiently. Most hydrogels are intelligently responsive to external stimuli, such as light, electric field, temperature, pH, magnetism, and so on [33]. These unique properties of hydrogel endow it with broad application prospects and great application values in printing and dyeing wastewater treatments. Due to the excellent properties of carbohydrate polymers, they have been used as the main materials to construct hydrogel skeletons [33].

In this study, we prepared Poly (TtEGDMA-cross-2-HPMA) hydrogels as a novel sorbent to remove ET_2 from aqueous solutions. Adsorption isotherm, the effect of initial dye concentration, and crosslinked agent were studied. The adsorption isotherms were fitted by Langmuir and Freundlich models. The adsorption was examined by using pseudo-first-order and pseudo-second-order kinetic models.

■ EXPERIMENTAL SECTION

Materials

Sorbent

The crosslinked agent, tetraethylene glycol dimethacrylate (TtEGDMA) ($C_{16}H_{26}O_7$) (MW = 330.38 g mol^{-1}) was supplied by Fluka, the monomer, 2-hydroxypropylmethancrylate (2-HPMA) (MW = 144.17 g mol^{-1}) was supplied by Merck-Schuchardt and the initiator, l'azobisisobutyronitrile (AIBN) was supplied by Merck, Darmstad, Germany. All chemicals were used as received. The mole number of 2-HPMA is 7×10^{-2} mol, and the concentration of 1, 5, and 10% of TtEGDMA are 7.1×10^{-4}, 3.55×10^{-3}, and 7.1×10^{-3} mol, respectively.

Sorbate

The basic cationic dye, bemacid red ($C_{14}H_{17}NSO_3Cl$) [34], was obtained from the silk production (SOITEX) Tlemcen industry (Algeria). The structure of this dye is displayed in Fig. 1. A 500 mg L^{-1} stock solution was prepared by dissolving the required amount of dye in distilled water. Working solutions of desired concentrations were obtained with successive dilutions.

Instrumentation

The samples were analyzed using FTIR spectroscopy IFS66 in 4000–400 cm^{-1}. Before the measurement, the samples were dried under a vacuum until reaching a constant weight. The dried samples were pressed into the powder, mixed with 10 times as much KBr powder, and then compressed to make a pellet for FTIR characterization.

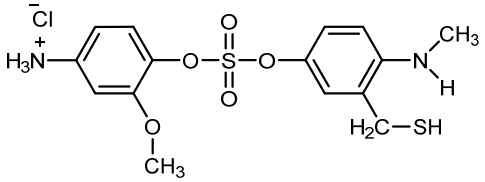

Fig 1. Chemical structure of bemacid red

The ^{13}C solid-state nuclear magnetic resonance spectra of Poly (TtEGDMA-cross-2-HPMA) were measured at 400 MHz on a Bruker MSL 300 spectrometer, using the cross-polarization/magic angle spinning (CP/MAS) probe with 4 mm O.D. rotors, under high power proton decoupling. The sample spinning was performed at 7.5 kHz, to easily recognize the sidebands. For each spectrum, 1000 scans were averaged using a recycling time of 4 s. The ^{13}C chemical shifts were calibrated in ppm relative to TMS by taking the ^{13}C chemical shift of the methine carbon of solid adamantane (29.5 ppm) as an external reference standard. All the measurements were performed at room temperature.

Procedure

Preparation of analytical method TtEGDMA-cross-2-HPMA

Poly (tetra (ethylene glycol) dimethacrylate-cross-2-hydroxypropyl methacrylate) materials, henceforth designated as Poly (TtEGDMA-cross-2-HPMA), were prepared by solution polymerization with a total concentration 10 wt.% (10.3 g of 2-HPMA). The concentration of 0.1 wt.% (0.1 g) was the initiator shown in Fig. 2. The free radical copolymerization was carried out under a nitrogen atmosphere in a three-necked flask equipped with a nitrogen inlet and a reflux condenser immersed in a constant temperature oil bath (yellow, ± 1 °C). The reaction mixture was stirred using a magnetic stirrer. A continuous supply of nitrogen was maintained throughout the reaction period. The solution polymerization proceeded for 24 h at 60 °C. Three various crosslinked Poly (TtEGDMA-cross-2-HPMA) samples were prepared with nominal crosslinking ratios, X, of 1, 5 and 10% mol TtEGDMA/mol 2-HPMA. Then, the copolymers obtained were washed by CH_2Cl_2 several times to extract unreacted monomers. The solid copolymer slab was cut into circular disks using punches.

Adsorption kinetics

Batch adsorption experiments were carried out at 25 °C by adding adsorbent (2.0 g) into several 300 mL glass Erlenmeyer flasks containing 200 mL solution of different initial concentrations (5, 10, 20, 30, 40, and 50 mg L^{-1}) of dye. The flasks were placed on a rotary shaker (120 rpm) in a thermostat. Agitation was provided for 240 min, which was more than sufficient to reach equilibrium. The samples (5 mL aliquot) were taken at suitable time intervals and centrifuged for 10 min at 3000 rpm. The ET_2 concentration in the supernatant solution was analyzed by measuring the optical density at 505 nm, using a spectrophotometer (Spectronic Genesys 5).

To investigate the kinetic mechanism, which controls the adsorption process of ET_2 on the hydrogel, the pseudo-first-order (PFO) [9,35] and pseudo-second-order (PSO) models were used to test the experiment data [9,35-37]. The pseudo-first-order kinetic model can

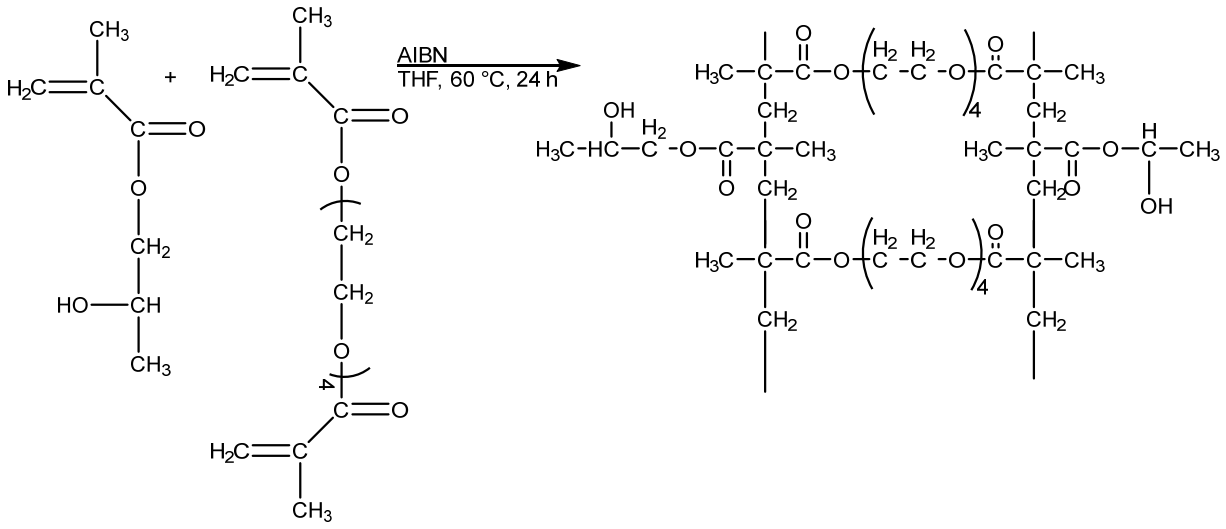

Fig 2. Chemical structure of Poly (TtEGDMA-cross-2-HPMA) hydrogel

be as Eq. (1). The pseudo-second-order model is based on the assumption of chemisorption of the adsorbate on the adsorbents. This model is given as Eq. (2):

$$Ln(q_e - q) = Lnq_e - \frac{k_{1,s}}{2.303}t \quad (1)$$

$$\frac{t}{q} = \frac{1}{k_{2,s}q_e^2} + \frac{1}{q_e}t \quad (2)$$

where, q_e is equilibrium adsorption capacity (mg g^{-1}), and $k_{1,s}$ is the pseudo-first-order rate constant (min^{-1}). The q_t parameter is the amount of adsorption dye (mg g^{-1}) at a time (min) while $k_{2,s}$ is the pseudo-second-order rate constant (min g mg^{-1}).

■ RESULTS AND DISCUSSION

Characterization of Copolymer

The FTIR spectra of poly (TtEGDMA-cross-2-HPMA) (a) 1% (b) 5% and (c) 10% TtEGDMA are shown in Fig. 3(a-c). It is observed that poly (TtEGDMA-cross-2-HPMA) spectra showed an absorption band typical at 1060 cm^{-1}, which is attributed to C–O [38-40], and the O–H bending vibrations 1006 cm^{-1} correspond to the HPMA comonomer of the copolymer. The ester stretching vibration (–C=O) of –COOR band at 1738 cm^{-1}, the C–O stretching at 1255 cm^{-1}. The other strong bands at 1450 correspond to the C–H bending (alkane, $–CH_3$, alkane, $–CH_2–$) of the alkane [41]. The FTIR shows C–O–C stretching peaks of the ester group of 1108 cm^{-1} [2,42], 1385 cm^{-1} due to the symmetrical deformation of its methyl (CH_3) [39] and deformation of the group CH–OH [43]. The absorption peak at 976 cm^{-1} corresponds to its $–CH_2–CH_2–O$ group vibration [2].

The ^{13}C-NMR spectrum of Poly (TtEGDMA-cross-2-HPMA) and its assignment are shown in Fig. 4. The α-methyl of TtEGDMA and 2-HPMA appeared at 18.8 ppm, the methylene of TtEGDMA and 2-HPMA appeared at 55.5 ppm. The signal due to the backbone methylene carbon of TtEGDMA is observed at 65.1 and 75 ppm, while the ester carbonyl of TtEGDMA and 2-HPMA appeared at 167 and 178.2 ppm, respectively.

Adsorption Studies

Fig. 5-6 shows experimental data, and the predicted curves for the sorption of ET_2 by Poly (TtEGDMA-cross-2-HPMA) using a linear method for the three hydrogels used models pseudo-second-order. Table 1 shows the pseudo-first and pseudo-second-order kinetic parameters for different initial concentrations of ET_2 obtained by utilizing the linear regression analysis method.

According to experimental data, a straight-line plot with a correlation coefficient of 0.995 suggests the applicability of the pseudo-first-order kinetics model to fit the experimental data (Table 1). The calculated value of adsorption capacity for 1% TtEGDMA for 50 mg g^{-1}, $q_{e,cal}$ (9.33 mg g^{-1}) is higher than the value of experimental adsorption capacity, $q_{e,exp}$ (9.25 mg g^{-1}). Therefore, the theoretical q_e values estimated from the

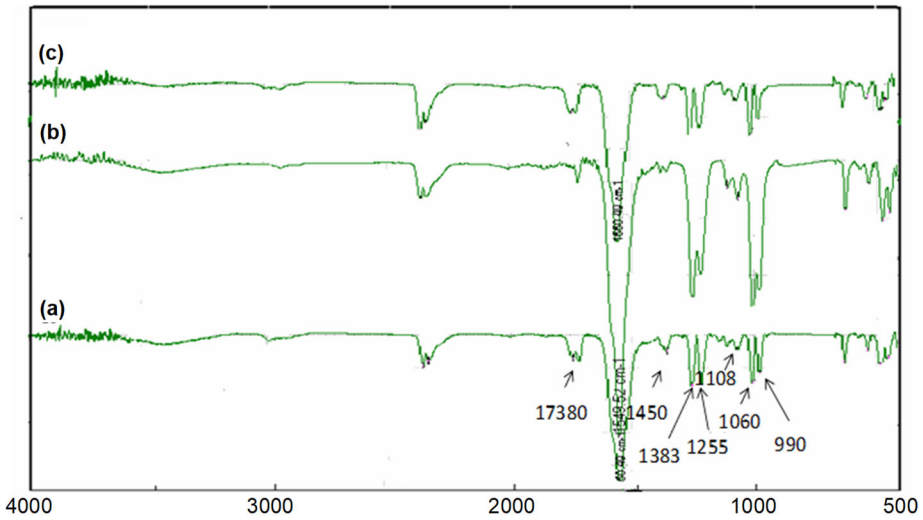

Fig 3. FTIR spectrum of Poly (TtEGDMA-cross-2-HPMA) hydrogels: (a) 1%, (b) 5% and (c)10% of TtEGDMA

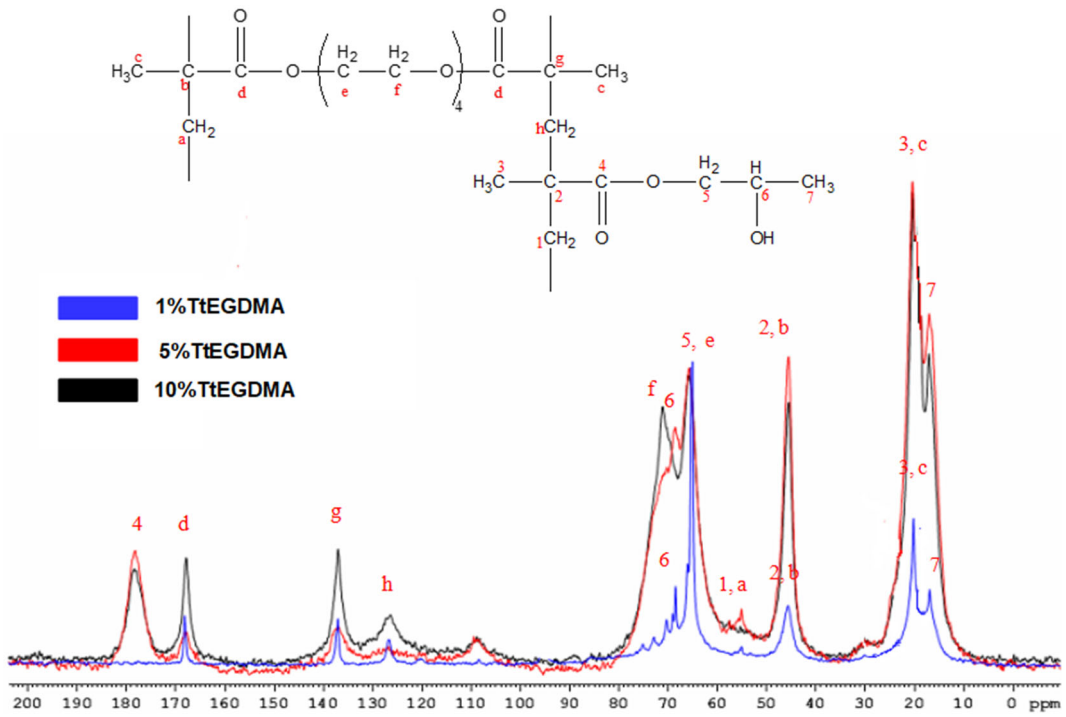

Fig 4. ^{13}C-NMR spectrum of Poly (TtEGDMA-cross-2-HPMA) hydrogels

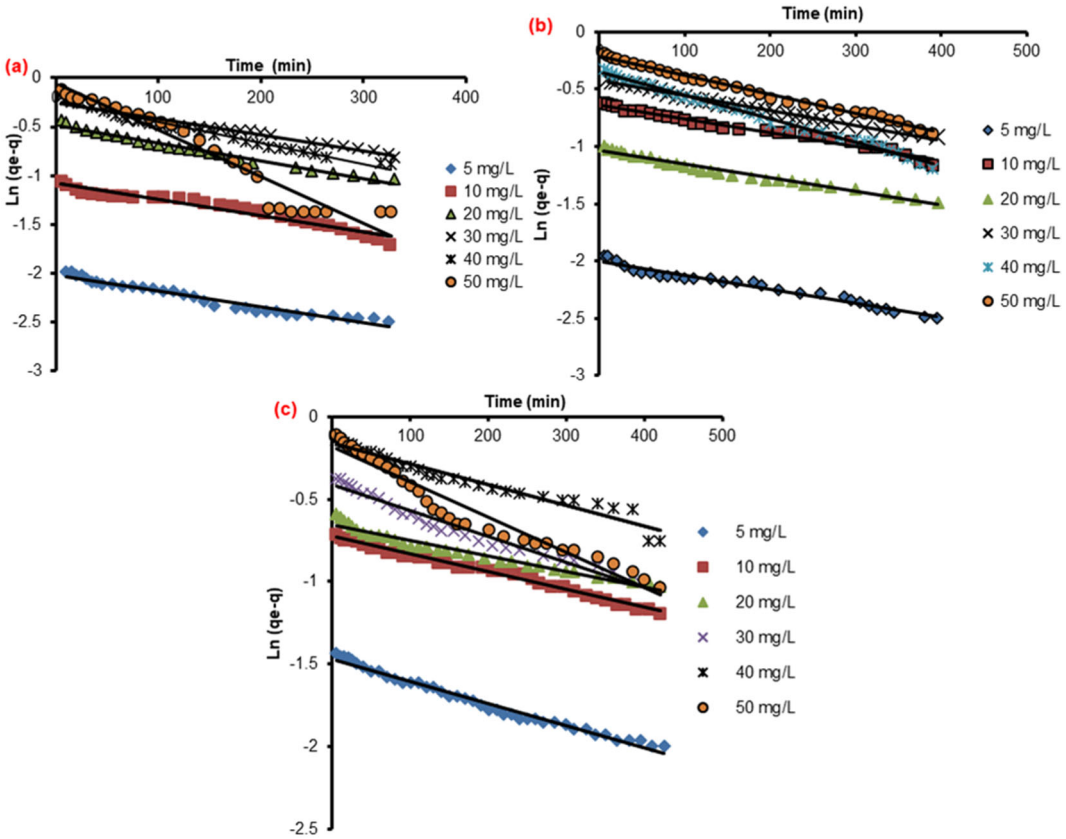

Fig 5. Pseudo-first order adsorption kinetics dyes of ET_2 by Poly (TtEGDMA-cross-2-HPMA) with (a) 1, (b) 5, and (c) 10% of TtEGDMA for various initial dye concentrations

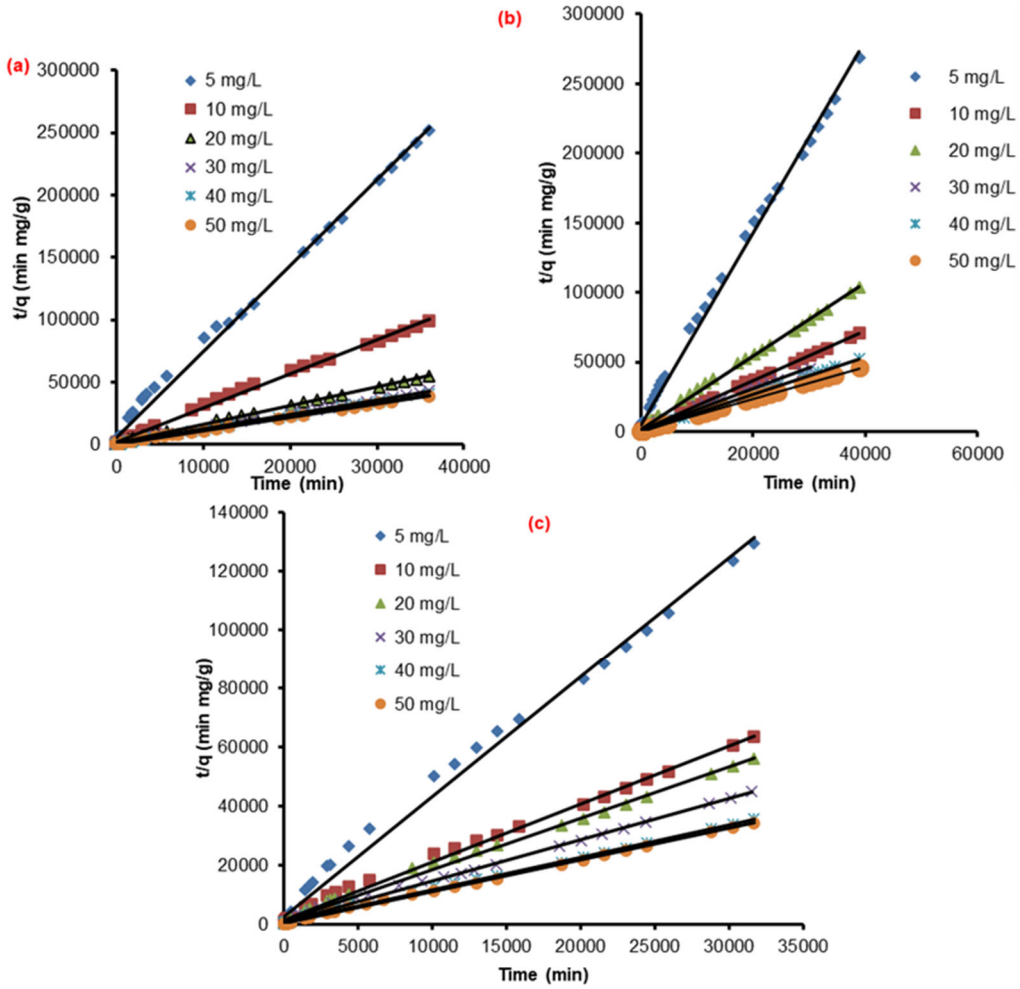

Fig 6. Pseudo-second order adsorption kinetics dyes of ET_2 by Poly (TtEGDMA-cross-2-HPMA) with (a) 1, (b) 5, and (c) 10% of TtEGDMA for various initial dye

Table 1. Calculated model parameters and regression coefficients for the pseudo-first-order and pseudo-second order for all studied concentration

TtEGDMA (% mol)	Concentration (mg L^{-1})	Pseudo first order			Pseudo second order			
		$k_{1,s}$ 10^2 (min^{-1})	$q_{e,cal}$ (mg g^{-1})	R^2	$k_{2,s}$ 10^4 (g mg^{-1} min^{-1})	$q_{e,cal}$ (mg g^{-1})	$q_{e,exp}$ (mg g^{-1})	R^2
1	5	3.76	1.81×10^{-9}	0.958	9.00	1.45	1.42	0.966
	10	3.86	2.20×10^{-5}	0.950	4.97	3.62	3.65	0.998
	20	4.23	8.00×10^{-3}	0.982	2.26	6.65	6.58	0.998
	30	3.81	8.30×10^{-2}	0.965	1.89	8.51	8.44	0.997
	40	4.97	9.60×10^{-2}	0.978	2.72	8.94	8.84	0.999
	50	1.99	5.59×10^{-1}	0.931	3.97	9.33	9.25	0.999
5	5	1.27	1.21×10^{-4}	0.963	2.03	0.65	0.65	0.997
	10	1.24	5.72×10^{-2}	0.975	8.02	1.71	1.69	0.998
	20	1.23	9.51×10^{-3}	0.980	5.06	2.52	2.48	0.999
	30	1.35	1.48×10^{-1}	0.992	4.01	3.05	3.02	0.998
	40	2.14	2.12×10^{-1}	0.994	8.20	3.37	3.33	0.999
	50	1.74	3.90×10^{-1}	0.993	5.92	3.87	3.82	0.999

Table 1. Calculated model parameters and regression coefficients for the pseudo-first-order and pseudo-second order for all studied concentration (*Continued*)

TtEGDMA (% mol)	Concentration (mg L^{-1})	Pseudo first order			Pseudo second order			
		$k_{1,s}$ 10^2 (min^{-1})	$q_{e,cal}$ (mg g^{-1})	R^2	$k_{2,s}$ 10^4 (g mg^{-1} min^{-1})	$q_{e,cal}$ (mg g^{-1})	$q_{e,exp}$ (mg g^{-1})	R^2
10	5	0.70	3.67×10^{-2}	0.981	26.6	0.55	0.55	0.995
	10	0.56	19.5×10^{-2}	0.990	10.3	1.14	1.12	0.996
	20	0.48	22.4×10^{-2}	0.980	10.4	1.29	1.27	0.996
	30	0.38	39.3×10^{-2}	0.961	9.50	1.60	1.58	0.997
	40	0.65	69.8×10^{-2}	0.952	6.30	2.04	1.99	0.997
	50	0.19	66.4×10^{-2}	0.949	13.2	2.09	2.07	0.999

first-order kinetic model gave significantly different values compared to experimental values comparing pseudo-second-order kinetic model, the correlation coefficient (R^2) of PSO model (0.996) is higher than that of PFO kinetic model (0.949) for ET_2, indicating that chemisorptions dominate the removal mechanism and due to the sharing or exchange of electrons of ET_2 [36,44-45]. These results showed that the first-order kinetic model did not describe these sorption systems. Thus, it could be suggested that the adsorption of ET_2 on hydrogel follows the pseudo-second-order better than the pseudo-first-order model. The pseudo-second-order kinetic model assumes that the rate-limiting step may be chemical adsorption. The rate-determining step may be chemical sorption involving valence forces through sharing or exchange of electrons between adsorbent and adsorbate. It may lead to the inference of a greater affinity and rapid bonding of ET_2 molecules to the surface of poly (TtEGDMA-cross-2-HPMA) [35,46].

Adsorption Isotherms

In this work, the most commonly used equilibrium isothermal models, Langmuir and Freundlich models, were adopted to simulate the adsorption isotherm of the prepared foams. Langmuir model is based on the assumption of a homogeneous adsorbent surface with identical adsorption sites, which can be expressed in Eq. (3) [36,47]:

$$q_e = \frac{q_0 \times b \times c_e}{1 + b \times c_e} \quad (3)$$

where, b is an equilibrium adsorption constant (L mg^{-1}), and q_0 is the saturated monolayer adsorption capacity (mg g^{-1}). A linearized plot of $1/q_e$ against $1/c_e$ gives a q_0 and b.

Freundlich adsorption isotherm describes the adsorption of adsorbates onto heterogeneous surfaces with different functional groups or adsorbent–adsorbate interactions as shown in Eq. (4) [36,48].

$$q_e = k_f \times c_e^{1/n} \quad (4)$$

This expression can be linearized to give:

$$\mathrm{Ln}q_e = \mathrm{Ln}k_f + \frac{1}{n}\mathrm{Ln}c_e \quad (5)$$

where, k_f and n are Freundlich constants, which represent adsorption capacity and adsorption intensity, respectively. K_f and n can be calculated from a linear plot of $\mathrm{Ln}q_e$ against $\mathrm{Ln}c_e$.

The calculated results of the Langmuir and Freundlich isotherm constants are given in Table 2. The R^2 of the Langmuir isothermal model for the ET_2 is 0.999, higher than those of the Freundlich isotherm model 0.959, demonstrating that the cationic dyes are

Table 2. Langmuir and Freundlich isotherm model constants and correlation coefficients

Hydrogel	TtEGDMA (% mol)	Langmuir model			Freundlich model		
		b	q_0	R^2	K_f 10^6	n	R^2
Poly (TtEGDMA-Cross-2-HPMA	1	953.16	0.13	0.999	9.26	0.18	0.959
	5	329.31	0.25	0.999	25.33	0.39	0.981
	10	48.39	0.85	0.999	208.88	1.03	0.959

Table 3. Comparing the adsorption capacities of the various hydrogels adsorbents towards ET_2 dye adsorption

Q_{max} (mg g^{-1})	Hydrogel adsorbent	Ref.
0.7	Poly (methacrylic acid-cross-dodecyleacrylate ammonium bromide)	[34]
0.159	Poly (acrylamide-cross-hydroxyethylmethacrylate)	[41]
0.85	Poly (TtEGDMA-cross-2-HPMA)	

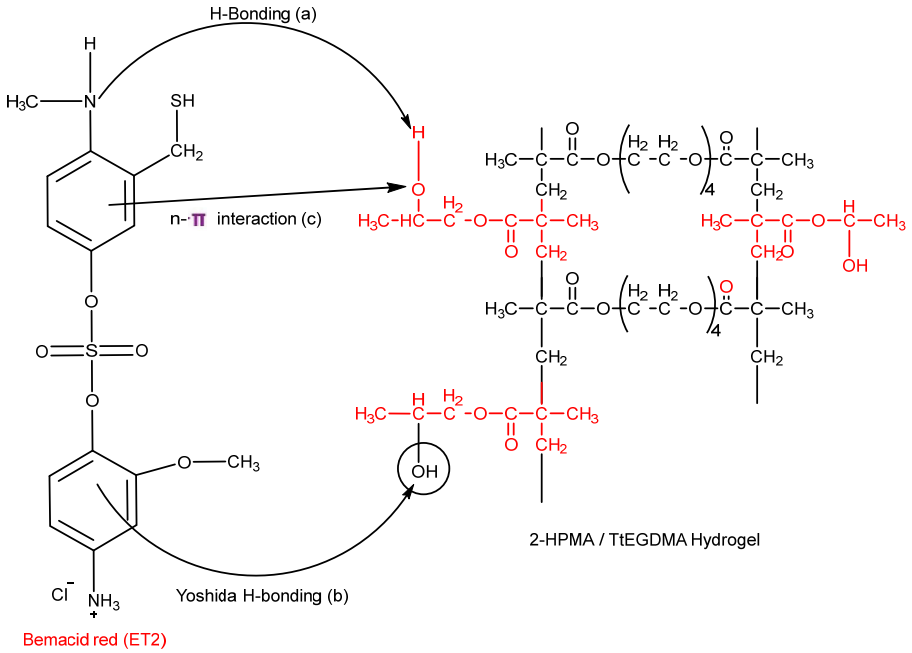

Fig 7. Proposed adsorption mechanisms of ET_2 on poly (TtEGDMA-cross-2-HPMA)

adsorbed in poly (TtEGDMA-cross-2-HPMA) a monolayer mode [36].

The adsorption capacity of Poly (TtEGDMA-cross-2-HPMA) towards ET_2 was compared with various types of hydrogel adsorbents reported in the literature, as recorded in Table 3. The results indicate a higher adsorption capacity than those used by other researchers.

Adsorption Mechanism

The proposed mechanisms for the adsorption of ET_2 dye onto poly (TtEGDMA-cross-2-HPMA) are illustrated in Fig. 7. Poly (TtEGDMA-cross-2-HPMA) contains a large number of hydroxyl functional groups, making it an ideal adsorbent for removing basic pollutants from the aqueous systems. Two types of hydrogen bonding interactions can occur in the 2-H system: (1) between hydroxyl groups (H-donor) on the poly (TtEGDMA-cross-2-HPMA) surface and H-acceptor atoms (i.e., nitrogen) in ET_2, and (2) between hydroxyl groups on the poly (TtEGDMA-cross-2-HPMA) surface and the aromatic rings in ET_2. The former is known as dipole–dipole H-bonding (Fig. 7(a)) and the latter is known as Yoshida H-bonding (Fig. 7(b)). The n-π interactions (also known as n-π electron donor–acceptor interactions) between oxygen groups on the poly (TtEGDMA-cross-2-HPMA) surface act as electron donors, while the aromatic rings of ET_2 act as electron acceptors (Fig. 7(c)) [35,49-50].

■ CONCLUSION

The potential of poly tetra (ethylene glycol) dimethacrylate-crosslinked-2-hyroxypropyl methacrylate) for the sorption of ET_2 from an aqueous solution was investigated. FTIR and ^{13}C-NMR confirmed the chemical structures. The effects of experimental parameters such as initial dye and crosslinked agent concentrations were studied. Initial dye concentration

and crosslinked agent concentration were found to have an influence on the sorption efficiency. Kinetic studies showed that the adsorption followed a pseudo-second-order kinetic model, indicating that chemical adsorption was the rate-limiting step. According to the best correlation results, the adsorption data of both hydrogels are found to fit well with the Langmuir isotherm. The dye adsorption mechanism onto hydrogels was electrostatic attraction, dipole-dipole hydrogen bonding, and Yoshida H-bonding. It can be concluded that Poly (TtEGDMA-cross-2-HPMA) is an alternative economic sorbent to more costly adsorbents used for dye removal in wastewater treatment processes.

■ ACKNOWLEDGMENTS

The authors acknowledge the research grant provided by The General Directorate for Scientific Research and Technological Development (PNR project) and the Ministry of Higher Education and Scientific Research of Algeria (Project No. E0182100066).

■ REFERENCES

[1] Santhi, T., Manonmani, S., Vasantha, S.V., and Chang, T.Y., 2016, A new alternative adsorbent for the removal of cationic dyes from aqueous solution, *Arabian J. Chem.*, 9, S466–S474.

[2] Bhattacharyya, R., and Ray, S.K., 2015, Removal of Congo red and methyl violet from water using nano clay filled composite hydrogels of poly acrylic acid and polyethylene glycol, *Chem. Eng. J.*, 260, 269–283.

[3] Ilgin, P., Ozay, H., and Ozay, O., 2019, Selective adsorption of cationic dyes from colored noxious effluent using a novel N-tert-butylmaleamic acid based hydrogels, *React. Funct. Polym.*, 142, 189–198.

[4] Yaseen, D.A., and Scholz, M., 2019, Textile dye wastewater characteristics and constituents of synthetic effluents: A critical review, *Int. J. Environ. Sci. Technol.*, 16 (2), 1193–1226.

[5] Khan, M., and Lo, I.M.C., 2016, A holistic review of hydrogel applications in the adsorptive removal of aqueous pollutants: Recent progress, challenges, and perspectives, *Water Res.*, 106, 259–271.

[6] Tran, V.V., Park, D., and Lee, Y.C., 2018, Hydrogel applications for adsorption of contaminants in water and wastewater treatment, *Environ. Sci. Pollut. Res.*, 25, 24569–24599.

[7] Pakdel, P.M., and Peighambardoust, S.J., 2018, A review on acrylic based hydrogels and their applications in wastewater treatment, *J. Environ. Manage.*, 217, 123–143.

[8] Titchou, F.E., Ait Akbour, R., Assabane, A., and Hamdani, M., 2020, Removal of cationic dye from aqueous solution using Moroccan pozzolana as adsorbent: Isotherms, kinetic studies, and application on real textile wastewater treatment, *Groundwater Sustainable Dev.*, 11, 100405.

[9] Wang, F., Li, L., Iqbal, J., Yang, Z., and Du, Y., 2022, Preparation of magnetic chitosan corn straw biochar and its application in adsorption of amaranth dye in aqueous solution, *Int. J. Biol. Macromol.*, 199, 234–242.

[10] Jawad, A.H., and Abdulhameed, A.S., 2020, Mesoporous Iraqi red kaolin clay as an efficient adsorbent for methylene blue dye: Adsorption kinetic, isotherm and mechanism study, *Surf. Interfaces*, 18, 100422.

[11] Munthalia, M.W., Johan, E., Aono, H., and Matsue, N., 2015, Cs^{+} and Sr^{2+} adsorption selectivity of zeolites in relation to radioactive decontamination, *J. Asian Ceram. Soc.*, 3 (3), 245–250.

[12] Niaei, H.A., and Rostamizadeh, M., 2020, Adsorption of metformin from an aqueous solution by Fe-ZSM-5 nano-adsorbent: Isotherm, kinetic and thermodynamic studies, *J. Chem. Thermodyn.*, 142, 106003.

[13] Brião, G.V., Jahn, S.L., Foletto, E.L., and Dotto, G.L., 2017, Adsorption of crystal violet dye onto a mesoporous ZSM-5 zeolite synthetized using chitin as template, *J. Colloid Interface Sci.*, 508, 313–322.

[14] Zhao, X., Zhao, H., Huang, X., Wang, L., Liu, F., Hu, X., Li, J., Zhang, G., and Ji, P., 2021, Effect and mechanisms of synthesis conditions on the cadmium adsorption capacity of modified fly ash, *Ecotoxicol. Environ. Saf.*, 223, 112550.

[15] Benvenuti, J., Fisch, A., dos Santos, J.H.Z., and Gutterres, M., 2019, Silica-based adsorbent material with grape bagasse encapsulated by the solgel method for the adsorption of Basic Blue 41 dye, *J. Environ. Chem. Eng.*, 7 (5), 103342.

[16] Raghav, S., Jain, P., and Kumar, D., 2022, Assembly of cerium impregnated pectin/silica–gel biopolymeric material for effective utilization for fluoride adsorption studies, *Mater. Today: Proc.*, 50, 273–281.

[17] Wang, D., Zhang, J., Yang, Q., Li, N., and Sumathy, K., 2014, Study of adsorption characteristics in silica gel–water adsorption refrigeration, *Appl. Energy*, 113, 734–741.

[18] Zhang, Y., Xia, K., Liu, X., Chen, Z., Du, H., and Zhang, X., 2019, Synthesis of cationic-modified silica gel and its adsorption properties for anionic dyes, *J. Taiwan Inst. Chem. Eng.*, 102, 1–8.

[19] Sadiq, A.C., Olasupo, A., Wan Ngah, W.S., Rahim, N.Y., and Mohd Suah, F.B., 2021, A decade development in the application of chitosan-based materials for dye adsorption: A short review, *Int. J. Biol. Macromol.*, 191, 1151–1163.

[20] Singh, A., Pal, D.B., Kumar, S., Srivastva, N., Syed, A., Elgorban, A.M., Singh, R., and Gupta, V.K., 2021, Studies on Zero-cost algae based phytoremediation of dye and heavy metal from simulated wastewater, *Bioresour. Technol.*, 342, 125971.

[21] Benafqir, M., Hsini, A Laabd, M., Laktif, T., Ait Addi, A., Albourine, A., and El Alem, N., 2020, Application of Density Functional Theory computation (DFT) and Process Capability Study for performance evaluation of orthophosphate removal process using Polyaniline@Hematite-titaniferous sand composite (PANI@HTS) as a substrate, *Sep. Purif. Technol.*, 236, 116286.

[22] Liu, C., Chen, X.X., Zhang, J., Zhou, H.Z., Zhang, L., and Guo, Y.K., 2018, Advanced treatment of bio-treated coal chemical wastewater by a novel combination of microbubble catalytic ozonation and biological process, *Sep. Purif. Technol.*, 197, 295–301.

[23] Zhou, L., Zhou, H., and Yang, X., 2019, Preparation and performance of a novel starch-based inorganic/organic composite coagulant for textile wastewater treatment, *Sep. Purif. Technol.*, 210, 93–99.

[24] Gupta, V.K., Tyagi, I., Agarwal, S., Singh, R., Chaudhary, M., Harit, A., and Kushwaha, S., 2016, Column operation studies for the removal of dyes and phenols using a low cost adsorbent, *Global J. Environ. Sci. Manage.*, 2, 1–10.

[25] Darwish, A.A.A., Rashad, M., and AL-Aoh, H.A., 2019, Methyl orange adsorption comparison on nanoparticles: Isotherm, kinetics, and thermodynamic studies, *Dyes Pigm.*, 160, 563–571.

[26] Mahmoud, G.A., Abdel-Aal, S.E., Badway, N.A., Elbayaa, A.A., and Ahmed, D.F., 2017, A novel hydrogel based on agricultural waste for removal of hazardous dyes from aqueous solution and reuse process in a secondary adsorption, *Polym. Bull.*, 74 (2), 337–358.

[27] Nasef, M.M., and Güven, O., 2012, Radiation-grafted copolymers for separation and purification purposes: Status, challenges and future directions, *Prog. Polym. Sci.*, 37 (12), 1597–1656.

[28] El Haouti, R., Ouachtak, H., El Guerdaoui, A., Amedlous, A., Amaterz, E., Haounati, R., Ait Addi, A., Akbal, F., El Alem, N., and Taha, M.L., 2019, Cationic dyes adsorption by Na-montmorillonite nano clay: Experimental study combined with a theoretical investigation using DFT based descriptors and molecular dynamics simulations, *J. Mol. Liq.*, 290, 111139.

[29] El-Zahhar, A.A., Awwad, N.S., and El-Katori, E.E., 2014, Removal of bromophenol blue dye from industrial waste water by synthesizing polymer-clay composite, *J. Mol. Liq.*, 199, 454–461.

[30] Fayazi, M., Afzali, D., Taher, M.A., Mostafavi, A., and Gupta, V.K., 2015, Removal of Safranin dye from aqueous solution using magnetic mesoporous clay: Optimization study, *J. Mol. Liq.*, 212, 675–685.

[31] Zhang, Z., Wang, W., Kang, Y., Zong, L., and Wang, A., 2016, Tailoring the properties of palygorskite by various organic acids *via* a one-pot hydrothermal process: A comparative study for removal of toxic dyes, *Appl. Clay Sci.*, 120, 28–39.

[32] Subbaiah, M.V., and Kim, D.S., 2016, Adsorption of methyl orange from aqueous solution by aminated pumpkin seed powder: Kinetics, isotherms, and thermodynamic studies, *Ecotoxicol. Environ. Saf.*, 128, 109–117.

[33] Chang, Z., Chen, Y., Tang, S., Yang, J., Chen, Y., Chen, S., Li, P., and Yang, Z., 2020, Construction of chitosan/polyacrylate/graphene oxide composite physical hydrogel by semi-dissolution/acidification/ sol-gel transition method and its simultaneous cationic and anionic dye adsorption properties, *Carbohydr. Polym.*, 229, 115431.

[34] Sebti, H., Fasla, A., and Ould Kada, S., 2015, Swelling properties of hydrogel networks of poly (methacrylic acid-cross-Nacrylate-N,N-dimethyl-N-dodecyl ammonium bromide). Application in the sorption of an industrial dye, *Pharma Chem.*, 7 (11), 17–25.

[35] Abd Malek, N.N., Jawad, A.H., Ismail, K., Razuan, R., and ALOthman, Z.A., 2021, Fly ash modified magnetic chitosan-polyvinyl alcohol blend for reactive orange 16 dye removal: Adsorption parametric optimization, *Int. J. Biol. Macromol.*, 189, 464–476.

[36] Ilgin, P., Ozay, H., and Ozay, O., 2019, Selective adsorption of cationic dyes from colored noxious effluent using a novel N-tert-butylmaleamic acid based hydrogels, *React. Funct. Polym.*, 142, 189–198.

[37] Tiwari, J.N., Mahesh, K., Le, N.H., Kemp, K.C., Timilsina, R., Tiwari, R.N., and Kim, K.S., 2013, Reduced graphene oxide-based hydrogels for the efficient capture of dye pollutants from aqueous solutions, *Carbon*, 56, 173–182.

[38] Bello, K., Sarojini, B.K., Narayana, B., Rao, A., and Byrappa, K., 2018, A study on adsorption behavior of newly synthesized banana pseudo-stem derived superabsorbent hydrogels for cationic and anionic dye removal from effluents, *Carbohydr. Polym.*, 181, 605–615.

[39] Bhattacharyya, R., and Ray, S.K., 2014, Micro- and nano-sized bentonite filled composite superabsorbents of chitosan and acrylic copolymer for removal of synthetic dyes from water, *Appl. Clay Sci.*, 101, 510–520.

[40] Maity, J., and Ray, S.K., 2014, Enhanced adsorption of methyl violet and Congo red by using semi and full IPN of polymethacrylic acid and chitosan, *Carbohydr. Polym.*, 104, 8–16.

[41] Bhattacharyya, R., Ray, S.K., and Mandal, B., 2013, A systematic method of synthesizing composite superabsorbent hydrogels from crosslink copolymer for removal of textile dyes from water, *J. Ind. Eng. Chem.*, 19 (4), 1191–1203.

[42] Bhattacharyya, R., and Ray, S.K., 2014, Enhanced adsorption of synthetic dyes from aqueous solution by a semi-interpenetrating network hydrogel based on starch, *J. Ind. Eng. Chem.*, 20 (5), 3714–3725.

[43] Pandey, S., Do, J.Y., Kim, J., and Kang, M., 2020, Fast and highly efficient removal of dye from aqueous solution using natural locust bean gum based hydrogels as adsorbent, *Int. J. Biol. Macromol.*, 143, 60–75.

[44] Bai, X., Gao, S., and Chen, W., 2014, The effect of anion $NO^{3-}/SO_4^{2-}/F^-$ on the optical performance and chroma index of glass coloured by cobalt, *Int. J. Microstruct. Mater. Prop.*, 9 (6), 525–531.

[45] Li, Y., Li, L., Chen, T., Duan, T., Yao, W., Zheng, K., Dai, L., and Zhu, W., 2018, Bioassembly of fungal hypha/graphene oxide aerogel as high performance adsorbents for U(VI) removal, *Chem. Eng. J.*, 347, 407–414.

[46] Baig, U., Uddin, M.K., and Gondal, M., 2020, Removal of hazardous azo dye from water using synthetic nano adsorbent: Facile synthesis, characterization, adsorption, regeneration and design of experiments, *Colloids Surf., A*, 584, 124031–124046.

[47] Li, R., An, Q.D., Xiao, Z.Y., Zhai, B., Zhai, S.R., and Shi, Z., 2017, Preparation of PEI/CS aerogel beads with a high density of reactive sites for efficient Cr(vi) sorption: Batch and column studies, *RSC Adv.*, 7 (64), 40227–40236.

[48] Cao, Q., Huang, F., Zhuang, Z., and Lin, Z., 2012, A study of the potential application of nano-$Mg(OH)_2$ in adsorbing low concentrations of uranyl tricarbonate from water, *Nanoscale*, 4 (7), 2423–2430.

[49] Jawad, A.H., Abd Malek, N.N., Abdulhameed, A.S., and Razuan, R., 2020, Synthesis of magnetic chitosan-fly ash/Fe_3O_4 composite for adsorption of reactive orange 16 dye: Optimization by Box–Behnken design, *J. Polym. Environ.*, 28 (3), 1068–1082.

[50] Abd Malek, N.N., Jawad, A.H., Abdulhameed, A.S., Ismail, K., and Hameed, B., 2020, New magnetic Schiff's base-chitosan-glyoxal/fly ash/Fe_3O_4 biocomposite for the removal of anionic azo dye: An optimized process, *Int. J. Biol. Macromol.*, 146, 530–539.